

## Constraining the prompt emission region and the ejecta speed of the distant GRB 220101A

---

Lorenzo Scotton,<sup>a,\*</sup> Frédéric Piron,<sup>a</sup> Nicola Omodei<sup>b</sup> and Niccolò Di Lalla<sup>b</sup> for the *Fermi*-LAT collaboration

<sup>a</sup>Laboratoire Universe et Particules de Montpellier, CNRS/IN2P3,  
Place Eugène Bataillon – CC 72, Montpellier, France

<sup>b</sup>Hansen Experimental Physics Lab, Stanford University,  
452 Lomita Mall, Stanford, California

E-mail: [lorenzo.scotton@lupm.in2p3.fr](mailto:lorenzo.scotton@lupm.in2p3.fr), [piron@in2p3.fr](mailto:piron@in2p3.fr),  
[nicola.omodei@stanford.edu](mailto:nicola.omodei@stanford.edu), [niccolo.dilalla@stanford.edu](mailto:niccolo.dilalla@stanford.edu)

GRB 220101A is the most distant gamma-ray burst detected by *Fermi*-LAT to date ( $z = 4.618$ ). It is a very energetic event, with an equivalent isotropic energy  $E_{iso} \sim 3.3 \times 10^{54}$  erg. We jointly analysed *Fermi*-GBM and LAT data with two analysis chains and obtained consistent results. They reveal a spectral break below 100 MeV in the LAT Low Energy (LLE) range during the prompt emission, associated with fast variability, which suggests that the spectral attenuation is caused by internal opacity to pair creation. Regardless of the nature of the emission processes, we find that the keV and MeV emissions were produced co-spatially above and close to the photosphere, with a moderate Lorentz factor  $\Gamma_{bulk} \sim 100$ . Here we present this study and compare our findings with other LAT-detected bursts with similar properties.

7th Heidelberg International Symposium on High-Energy Gamma-Ray Astronomy (*Gamma2022*)  
4-8 July 2022  
Barcelona, Spain

---

\*Speaker

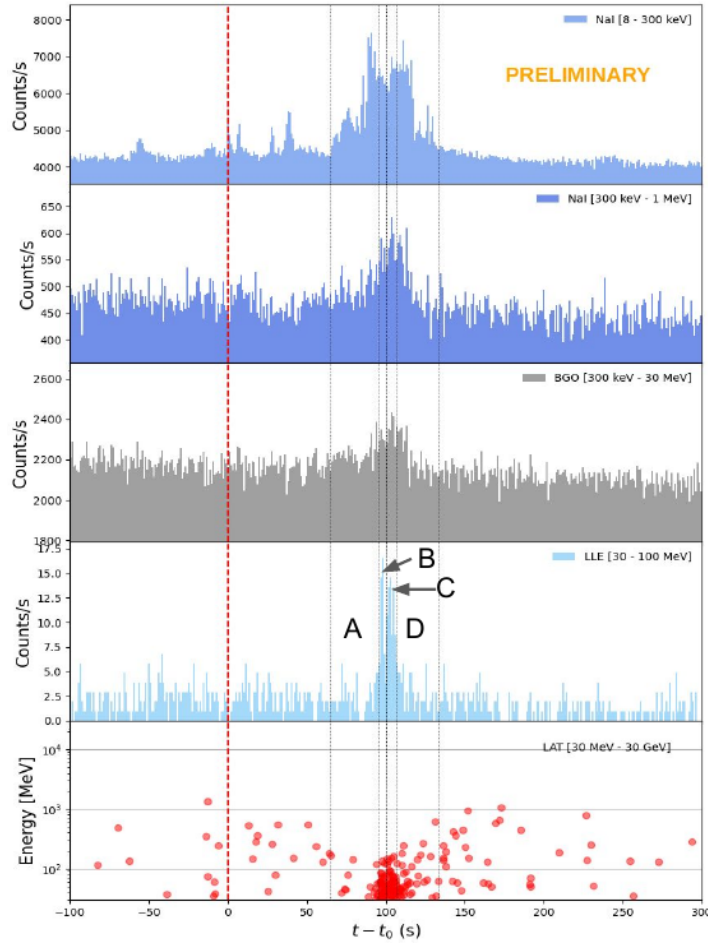


**Figure 1:** *Fermi* multi-detector light curve of GRB 220101A prompt emission in increasing energy bands from the top panel to the bottom panel. The red dashed vertical line denotes the time of the trigger, while the black dashed vertical lines indicate the time intervals chosen for the time-resolved spectral analysis, covering the main emission episode observed by the LAT.

## 1. Observations

The *Fermi*-GBM triggered on GRB 220101A at 05:10:11.51 UT on January 1, 2022 [1]. The burst was also detected by the *Fermi*-LAT at high energies [2]. The LAT on-ground localization of the event is RA, Dec =  $1.52^\circ$ ,  $31.75^\circ$  with an error radius of  $0.46^\circ$ . GRB 220101A is the most-distant LAT-detected burst to date with a redshift  $z = 4.618$  [3]. In this work we used the GBM Time Tagged Events (TTE) recorded by the NaI detectors 3, 6, 7, 9, and by the BGO detector 1. We used the LAT standard P8R3\_TRANSIENT020E\_V2 data, and additionally the LAT Low Energy (LLE [4]) data to extend our analysis down to 20 MeV. Figure 1 shows the *Fermi* multi-detector light curve of GRB 220101A during its prompt emission ( $T_{90} \sim 128$  s [1]). Interestingly, the high-energy flux is attenuated above  $\sim 100$  MeV during the brightest emission episode around  $T_0 + 100$  s (time bins B and C).

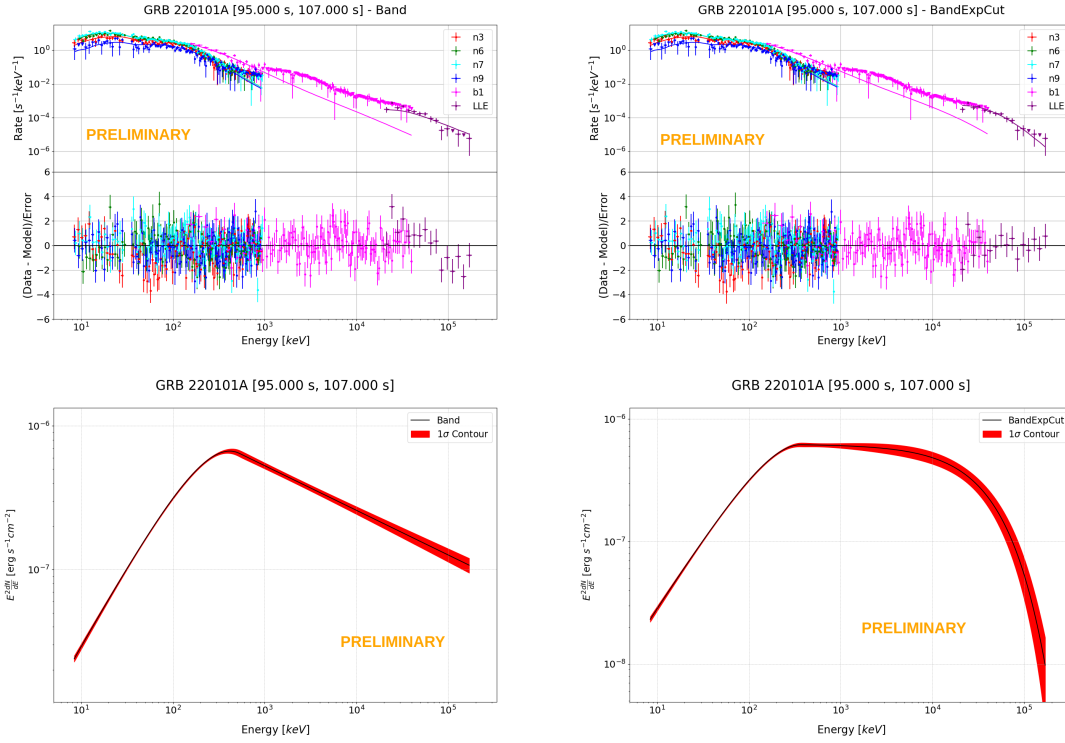


**Figure 2:** Left: GRB count spectra and residuals (upper panel) and SED (lower panel) from Band fits to GBM+LLE data in time bin B+C with pyXSPEC. Right: same for BandExpCut model, obtained by multiplying the Band function by a high-energy exponential cutoff.

## 2. Analysis procedure

We jointly analysed GBM and LLE data with the pyXSPEC fitting software<sup>1</sup>. We also performed a joint spectral analysis using the “Multi-Mission Maximum Likelihood” (threeML) software<sup>2</sup>[7], which combines simultaneously the native likelihoods of different instruments. In this analysis, threeML offered the full accuracy of the LAT unbinned likelihood technique, which is lost during the binning in space and energy that is required by pyXSPEC. We considered the spectral models Band [5] and ISSM [6], both having four parameters. Additionally, we considered the models obtained by multiplying these functions by a high-energy exponential cutoff ( $\propto e^{-E/E_{cut}}$ ). We called the resulting models BandExpCut and ISSMExpCut.

## 3. Spectral analysis results

We fitted BandExpCut to GBM+LLE data and found a significant cutoff  $E_{cut} = 22 \pm 8$  MeV in time bin B,  $70 \pm 24$  MeV in time bin C, and  $41 \pm 12$  MeV in time bin B+C. Figure 2 shows the GRB count spectra, residuals, and SEDs when fitting Band (left panels) and BandExpCut (right panels) to GBM+LLE data in time bin B+C. We checked that the results did not depend strongly on the specific

<sup>1</sup><https://heasarc.gsfc.nasa.gov/xanadu/xspec/python/html/index.html>

<sup>2</sup><https://threeML.readthedocs.io/en/latest/index.html>

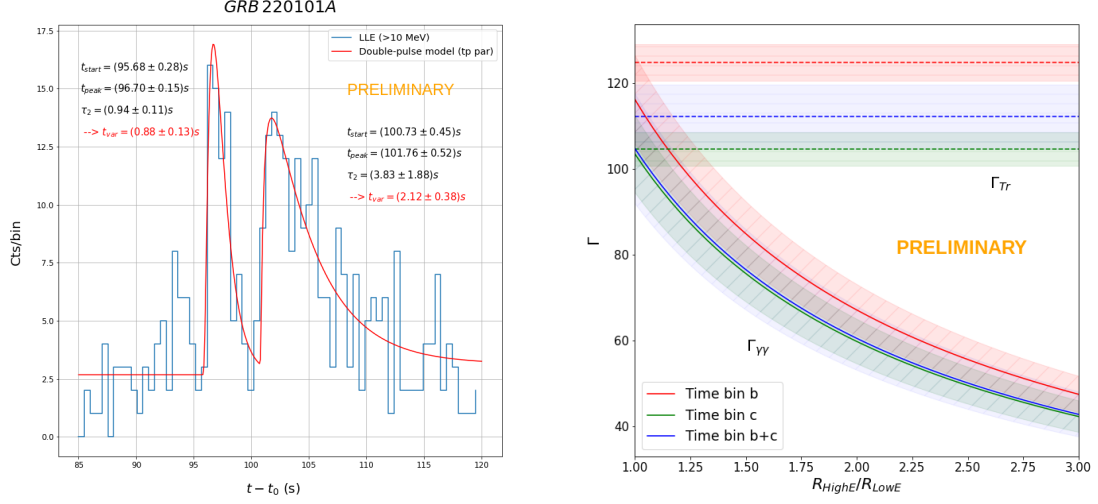


**Figure 3:** Left: light curve showing the two LLE peaks with the best-fit function superimposed. Right:  $\Gamma_{\gamma\gamma}$  and  $\Gamma_{Tr}$  as function of the ratio of the radii at which the high and low-energy emissions were produced in time bins B, C, and B+C.

choice of the Band model, then we also used the ISSM model to describe the non-thermal spectrum. When fitting ISSMExpCut a high-energy cut was detected only in time bin B at  $40 \pm 10$  MeV and with a smaller significance. This is explained by the continuous curvature of ISSM, which reflects the natural shape of GRB synchrotron spectra, and accounts for part of the spectral attenuation at high energies. The spectral results obtained with threeML are fully consistent with the pyXSPEC analysis, confirming the cutoff detections. We performed the same fits on GBM+LLE+LAT data, limiting LLE data below 100 MeV, and considering the LAT standard data above 100 MeV. We detected spectral cutoffs in time bins B, C, and B+C with both BandExpCut and ISSMExpCut functions at values compatible within errors with the previous analyses.

## 4. Interpretation

The temporal variability observed at high-energy suggests that the spectral cutoffs are due to gamma opacity to pair creation. We estimated the minimum variability time scale of the high-energy emission and we coupled it with the detected cutoffs to determine the speed of the jet and to localize the region in which all of the high-energy emission was produced [8][9].

### 4.1 Estimate of the variability time scale

We considered the Fast Rise Exponential Decay function to estimate the minimum variability time scale  $t_{\text{var}}$ , and we modified it to fit simultaneously the two main LLE peaks. On each peak the

function reads:

$$I(t) = \begin{cases} B, & \text{if } t \leq t_{start} \\ A \times \exp \left\{ -\frac{1}{\tau_2} \left[ \frac{(t_{peak} - t_{start})^2}{t - t_{start}} + (t - t_{start}) \right] \right\} + B, & \text{otherwise} \end{cases} \quad (1)$$

The left panel of [Figure 3](#) shows the two LLE peaks superimposed to the best-fit function.  $t_{var}$  of each pulse is estimated as the half-width at half-maximum, and it is  $0.88 \pm 0.13$  s in the first peak, and  $2.12 \pm 0.38$  s in the second peak.

#### 4.2 Bulk Lorentz factor and localization of the prompt emission region

The bulk Lorentz factor  $\Gamma_{\gamma\gamma}$  is obtained as in [9] assuming that the observed spectral cutoff is due to opacity to pair creation in the GRB jet, and that the prompt emission is produced near or above the photosphere at a radius  $R_{LE}$  for the low-energy emission and  $R_{HE}$  for the high-energy emission [8].

$$\Gamma_{\gamma\gamma} = \frac{K\Phi(s)}{\left[ \frac{1}{2} \left( 1 + \frac{R_{HE}}{R_{LE}} \right) \left( \frac{R_{HE}}{R_{LE}} \right) \right]^{1/2}} (1+z)^{-(1+s)/(1-s)} \times \left\{ \sigma_T \left[ \frac{D_L(z)}{ct_{var}} \right]^2 E_* F(E_*) \right\}^{1/2(1-s)} \left[ \frac{E_* E_{cut}}{(m_e c^2)^2} \right]^{(s+1)/2(s-1)} \quad (2)$$

where  $E_*$  is the typical energy of the photons interacting with those at the cutoff energy,  $s$  is the photon index of the seed spectrum close to  $E_*$ , and  $F(E_*)$  is the photon fluence at  $E_*$  integrated over  $t_{var}$ .  $\Gamma_{\gamma\gamma}$  accounts for the redshift of the source too. The photospheric radius  $R_{ph}$  at which the jet becomes transparent to Thomson scattering, as well as the minimal bulk Lorentz factor  $\Gamma_{Tr}$  defining this transparency condition are computed as in [9]. The right panel of [Figure 3](#) shows the value of  $\Gamma_{\gamma\gamma}$  and  $\Gamma_{Tr}$  as a function of the radii at which the high and low-energy emissions were produced. When the high and low-energy emission are co-spatial then  $\Gamma_{\gamma\gamma}$  and its contour are comparable or greater than  $\Gamma_{Tr}$ . The transparency condition is thus fulfilled. We conclude that  $\Gamma_{bulk} \sim 100$  and that all of the high-energy emission took place near or above the photosphere at a radius of few  $10^{14}$  cm, typical of internal shocks.

#### 5. Discussion and conclusions

A total of 5 LAT-detected GRBs are known for presenting a spectral cutoff at high energies. For GRB 090926A [9] and GRB 220101A,  $\Gamma_{bulk}$  was estimated following the procedure presented in the previous section. For GRB 100724B and GRB 160509A, [10] estimated  $\Gamma_{bulk}$  between 100 – 400 adopting the internal shock model of [12] and the photospheric one of [13]. For GRB 170405A, [11] estimated a lower limit of  $\Gamma_{bulk} = 170$  [12] and an upper limit of 420 [14]. The value of  $\Gamma_{bulk}$  is order of few  $\sim 100$  in all cases. These GRBs represent a precious set in which a direct estimation of  $\Gamma_{bulk}$  can be performed.

#### Acknowledgements

The *Fermi*-LAT Collaboration acknowledges support for LAT development, operation and data analysis from NASA and DOE (United States), CEA/Irfu and IN2P3/CNRS (France), ASI

and INFN (Italy), MEXT, KEK, and JAXA (Japan), and the K.A. Wallenberg Foundation, the Swedish Research Council and the National Space Board (Sweden). Science analysis support in the operations phase from INAF (Italy) and CNES (France) is also gratefully acknowledged. This work performed in part under DOE Contract DE-AC02-76SF00515.

## References

- [1] Lesage, S. et al, *GRB 220101A: Fermi GBM Detection* (2022), GRB Coordinates Network
- [2] Arimoto, M. et al., *GRB 220101A: Fermi-LAT detection* (2022), GRB Coordinates Network
- [3] Fu, S. Y. et al., *GRB 220101A: Xinglong-2.16m photometry and spectroscopy* (2022), GRB Coordinates Network
- [4] Pelassa, V. et al., *The LAT Low-Energy technique for Fermi Gamma-Ray Bursts spectral analysis* (2010), Proceedings for the 2009 *Fermi Symposium*
- [5] Band, D. et al., *BATSE observations of gamma-ray burst spectra. I - Spectral diversity* (1993), *The Astrophysical Journal*
- [6] Yassine, M. et al., *A new fitting function for GRB MeV spectra based on the internal shock synchrotron model* (2020), *Astronomy & Astrophysics*
- [7] Vianello, G. et al., *The Multi-Mission Maximum Likelihood framework (3ML)* (2015), Proceedings of the 34th International Cosmic Ray Conference
- [8] Hascoët, R. et al., *Do Fermi Large Area Telescope observations imply very large Lorentz factors in gamma-ray burst outflows?* (2012), *Monthly Notices of the Royal Astronomical Society*
- [9] Yassine, M. et al., *Time evolution of the spectral break in the high-energy extra component of GRB 090926A* (2017), *Astronomy & Astrophysics*
- [10] Vianello, G. et al., *The Bright and the Slow—GRBs 100724B and 160509A with High-energy Cutoffs at  $\lesssim 100$  MeV* (2018), *The Astrophysical Journal*
- [11] Arimoto, M. et al., *Physical Origin of GeV Emission in the Early Phase of GRB 170405A: Clues from Emission Onsets with Multiwavelength Observations* (2020), *The Astrophysical Journal*
- [12] Granot, J. et al., *Opacity Buildup in Impulsive Relativistic Sources* (2008), *The Astrophysical Journal*
- [13] Gill, R. et al., *Non-thermal Gamma-Ray Emission from Delayed Pair Breakdown in a Magnetized and Photon-rich Outflow* (2014), *The Astrophysical Journal*
- [14] Gill, R. and Granot, J., *The effect of pair cascades on the high-energy spectral cut-off in gamma-ray bursts* (2018), *Monthly Notices of the Royal Astronomical Society*